Recombinant truncated TGF-β receptor II attenuates carbon tetrachloride-induced epithelial-mesenchymal transition and liver fibrosis in rats

LUXIN LI, HONGZHI LI, ZHEN ZHANG, JUNYA ZHENG, YONGPING SHI,
JIETING LIU, YANAN CAO, XIAOHUAN YUAN and YANHUI CHU

Heilongjiang Key Laboratory of Anti-Fibrosis Biotherapy, Mudanjiang Medical University,
Mudanjiang, Heilongjiang 157011, P.R. China

Abstract. Liver fibrosis is a pathological process of chronic liver diseases. In particular, epithelial-mesenchymal transition (EMT) is a major source of myofibroblast structure in liver fibrosis. The present study investigated the effects of recombinant truncated transforming growth factor-ß receptor II (rtTGFβRII) on EMT and liver fibrosis in a carbon tetrachloride (CCl_4)-induced rat model. A total of 24 rats were randomly separated into three groups: Normal control (NC), model (CCl_4) and treatment (CCl_4 + rtTGFβRII) groups. Histological methods, including hematoxylin and eosin, Masson's trichrome and Sirius red staining were conducted. The activities of serum alanine aminotransferase (ALT) and aspartate aminotransferase (AST) were measured using an automatic biochemical analyzer. The mRNA expression levels of fibroblast specific protein-1 (FSP-1), α-smooth muscle actin (α-SMA), fibronectin, collagen I, vimentin and E-cadherin were detected using reverse transcription-quantitative polymerase chain reaction analysis. The protein levels of fibronectin, collagen I, E-cadherin, Smad2/3 and phosphorylated (p)-Smad2/3 were detected using western blot analysis. The expression of α-SMA, fibronectin, vimentin and E-cadherin in the liver tissue was detected using immunofluorescence staining. The results demonstrated that *in vivo*, rtTGFβRII significantly reduced the degree of liver injury, serum ALT and AST activities and liver fibrosis. These factors were associated with reduced expression of FSP-1, α-SMA, fibronectin, collagen I, vimentin and p-Smad2/3, and increased expression of E-cadherin. The results of the present study suggest that rtTGFβRII may inhibit EMT processes in CCl_4-induced liver fibrosis in rats and alter the expression of epithelial and myofibroblast markers. Therefore, rtTGFβRII may be considered a possible treatment for preventing liver fibrosis via EMT processes.

Introduction

Liver fibrosis is a complex pathophysiological process characterized by the production and excessive deposition of extracellular matrix (ECM) (1-3), leading to loss of liver function, remodeling of liver blood vessels and destruction of liver structures. Liver fibrosis is generally considered a reversible wound healing response following liver injury. This process occurs in all chronic liver diseases, and can eventually lead to irreversible cirrhosis and liver failure (4,5); therefore preventing and reversing liver fibrosis is a primary measure for the treatment of liver diseases (6).

Epithelial-mesenchymal transition (EMT) refers to a process in which epithelial cells lose their typical epithelial properties and become motile as mesenchymal cells (7). The EMT process is accompanied by a loss of epithelial characteristics, including E-cadherin expression, and an increase in mesenchymal cells and fibroblast markers, including α-smooth muscle actin (α-SMA) (8,9). EMT has been reported to be associated with liver fibrosis. Previous studies have suggested that activation of collagen-producing myofibroblasts can be enhanced by hepatocytes and biliary epithelial cells via EMT during liver fibrosis (10,11), which can result in excessive deposition of ECM in the liver (12).

Transforming growth factor-β (TGF-β) is a principal profibrotic cytokine (13), which can induce EMT during liver fibrosis. It has previously been suggested that EMT is regulated by various profibrotic cytokines, with TGF-β1 considered the most important (14). TGF-β1 has been reported to initiate and finalize EMT processes in animal disease models and patients (15). Growing evidence has indicated that the prevention of EMT development may control and reverse liver fibrosis (16).

Correspondence to: Professor Yanhui Chu or Professor Xiaohuan Yuan, Heilongjiang Key Laboratory of Anti-Fibrosis Biotherapy, Mudanjiang Medical University, 3 Tongxiang Road, Mudanjiang, Heilongjiang 157011, P.R. China
E-mail: yanhui_chu@sina.com
E-mail: yuanxiaohuan1969@163.com

Blocking TGF-β signal transduction and understanding the mechanism underlying EMT has great significance for the development of novel effective therapies for the treatment of EMT-associated fibrosis diseases (17). A novel truncated (27-123 residues) type II TGF-β receptor (tTGFβRII) was designed and constructed, which works as a dominant-negative receptor. A previous study demonstrated that recombinant tTGFβRII (rtTGFβRII) can efficiently trap TGF-β1 from access to wild-type receptors and can prevent TGF-β1-triggered signals (18). Therefore, the present study aimed to determine whether rtTGFβRII ameliorates liver fibrosis by inhibiting EMT.

Materials and methods

Expression and purification of rtTGFβRII protein. The tTGFβRII sequence was amplified by reverse transcription-polymerase chain reaction (RT-PCR) and cloned into the pET-28a vector prior to transformation into *Escherichia coli* BL21 cells. Briefly, the tTGFβRII sequence was synthesized from the RNA of human peripheral blood using the Catrimox-14 reagent (Takara Biotechnology, Co., Ltd., Dalian, China). Informed consent was obtained for the collection of blood sample from a healthy volunteer, and this study was approved by the Ethics Committee of Mudanjiang Medical University (Mudanjiang, China). The total RNA (1 μg) was reverse transcribed to cDNA using the First-Strand cDNA Synthesis kit (Roche Diagnostics, Indianapolis, IN, USA) according to the manufacturer's protocol. The 10X polymerase chain reaction buffer and dNTP mixture were purchased from Takara Biotechnology Co., Ltd. The primers (synthesized by Sangon Biotech Co., Ltd., Shanghai, China), were as follows: Forward, 5'-CCGGAATTCCACGTTCAGAAGTCGGTT AA-3' and reverse, 5'-TTGCGGCCGCCATAATGCACTTTG GAGAAG-3'. The PCR conditions were as follows: 94°C for 5 min, 30 cycles of 94°C for 30 sec, 55°C for 30 sec and 72°C for 30 sec, and a final extension of 72°C for 10 min.

The recombinant plasmid pET-28a/tTGFβRII contained 6 histidine tags, and was grown overnight in lysogeny broth (LB) medium that contained 50 μg/ml kanamycin at 37°C, with agitation at 210 rpm. Subsequently, the culture was diluted 1:100 in fresh LB medium that contained 50 μg/ml kanamycin and was cultured at 37°C until optical density at 600 nm values of the media reached 0.6. Afterwards, 1 mmol/l isopropyl β-D-thiogalactopyranoside was added for induction at 37°C and the cells were harvested after 12 h. Purification was completed using Ni-NTA agarose affinity chromatography. The expression and purity of rtTGFβRII was analyzed by 15% SDS-PAGE with Coomassie brilliant blue staining. The purified recombinant protein was measured using a bicinchoninic acid (BCA) protein assay kit according to the manufacturer's protocol and stored at -80°C until further use.

Animals and treatment. All experimental protocols were approved by the Mudanjiang Medical University Animal Care and Veterinary Services Committee (Mudanjiang, China). The methods were carried out in accordance with the Guidelines for the Care and Use of Laboratory Animals (19). A rat model of liver fibrosis was induced using carbon tetrachloride (CCl$_4$). A total of 24 male Sprague Dawley rats (age, 10 weeks; weight, 200-250 g) were obtained from the SLAC Laboratory Animal Co., Ltd. (Shanghai, China). The animals were maintained under a 12 h light/dark cycle at 22°C with free access to food and water. After acclimation for 1 week, the rats were randomly divided into three groups (n=8 rats/group): Normal control (NC), model (CCl$_4$), and treatment (CCl$_4$ + rtTGFβRII) groups. The NC group received an intraperitoneal (i.p.) injection of 2 ml/kg body weight (b.w.) pure olive oil twice a week for 8 weeks and were then administered 2 ml/kg b.w. pure olive oil (i.p.) once a week for 4 weeks. The CCl$_4$ group received 2 ml/kg b.w., CCl$_4$ solution (40% CCl$_4$ in pure olive oil, i.p.) twice a week for 8 weeks and afterwards were administered a CCl$_4$ solution 2 ml/kg b.w. once a week for 4 weeks. The treatment group (CCl$_4$ + rtTGFβRII) received 2 ml/kg b.w. CCl$_4$ solution (40% CCl$_4$ in pure olive oil, i.p.) twice a week for 8 weeks and once a week for 4 weeks. Once the rats had been treated for 8 weeks they were administered 1 mg/kg b.w. rtTGFβRII (i.p.), two times a week, over a total of 4 weeks. All of the rats were sacrificed under anesthesia with an i.p. injection of 10% chloral hydrate (3 ml/kg b.w.), and blood and liver samples were collected. Blood samples were centrifuged at 1,500 x g for 10 min at 4°C to separate serum; the serum activities of ALT and AST were then detected by the Hongqi Hospital of Mudanjiang Medical University using a fully automatic biochemical analyzer (AU640; Olympus Corporation, Tokyo, Japan). A portion of the liver was immediately fixed in 10% formalin for histological analyses. The rest of the liver tissue was rapidly frozen and maintained at -80°C until assessed. Liver samples were acquired for analyses of liver function, and the detection of mRNA and protein expression levels of fibrosis-associated factors by RT-quantitative (q)PCR, histology, immunofluorescence and western blot analysis.

RNA extraction and RT-qPCR analysis. Total RNA was extracted using TRIzol reagent (Invitrogen; Thermo Fisher Scientific, Inc., Waltham, MA, USA) according to the manufacturer's protocol. Total RNA (1 μg) was reverse transcribed to cDNA using the First-Strand cDNA Synthesis kit (Roche Diagnostics) according to the manufacturer's instructions. Gene expression was measured by RT-qPCR using a SYBR Green RT-qPCR Master Mix and a StepOne Real-time PCR system (Applied Biosystems; Thermo Fisher Scientific, Inc.). The thermocycling conditions were as follows: 95°C for 10 min, followed by 40 cycles of 95°C for 15 sec and 60°C for 1 min. PCR primer sequences were as follows: β-actin forward, 5'-GGAGATTAC TGCCCTGGCTCCTA-3' and reverse, 5'-GACTCATCGTAC TCCTGCTTGCTG-3'; vimentin forward, 5'-TGACATTGA GATCGCCACCT-3' and reverse, 5'-TCATCGTGGTGCTGA GAAGT-3'; fibroblast-specific protein (FSP-1) forward, 5'-ATG TAATAGTGTCCACCTTCC-3' and reverse, 5'-ACTTCA TTGTCCCTGTTGCT-3'; fibronectin forward, 5'-CCGAAT CACAGTAGTTGCGG-3' and reverse, 5'-GCATAGTGTCCG GACCGATA-3'; E-cadherin forward, 5'-TCATCACAGACC CCAAGACC-3' and reverse, 5'-GATCTCCAGACCCACACC AA-3'; collagen I forward, 5'-CTGCTGGTGAGAGAGGTG AA-3' and reverse, 5'-GGAAACCTCTCTCGCCTCTT-3'; and α-smooth muscle actin (α-SMA) forward, 5'-CATCATGCG TCTGGACTTGG-3' and reverse, 5'-CCAGGGAAGAAGAGG AAGCA-3'. β-actin was used as an internal control and relative

quantification of gene expression was performed using the $2^{-\Delta\Delta Cq}$ method (20).

Histological analysis. The liver tissues were fixed in 10% neutraformaline for 24 h at room temperature and were embedded in paraffin. Tissue sections (5 μm) underwent hematoxylin and eosin (H&E), Masson's trichrome (MTS; cat no. D026; Nanjing Jiancheng Bioengineering Institute, Nanjing, China) and Sirius red staining (cat no. ab150681; Abcam, Cambridge, MA, USA) to study morphological alterations. All histological analyses were performed according to the manufacturer's instructions. For semi-quantitative morphometry, fibrotic areas stained with MTS and Sirius red staining were detected and calculated with ImageJ v1.42q software [National Institutes of Health (NIH), Bethesda, MD, USA] in eight randomly selected micrographs.

Immunofluorescence staining. Immunofluorescence analysis was performed on 5 μm liver sections that were dewaxed with xylene and hydrated using sequential ethanol and distilled water. The sections were permeabilized in 0.1% Triton X-100/PBS for 10 min, blocked with 1% bovine serum albumin (BSA)/PBS containing 0.1% Tween (both from Beijing Solarbio Science & Technology Co., Ltd., Beijing, China) for 60 min at room temperature and were incubated with antibodies against E-cadherin (1:100 dilution; cat no. sc-7870), fibronectin (1:100 dilution; cat no. sc-69682) (both from Santa Cruz Biotechnology, Inc., Dallas, TX, USA), α-SMA (1:200 dilution; cat. no. ab5694; Abcam) and vimentin (1:100 dilution; cat. no. sc-7558; Santa Cruz Biotechnology, Inc.) at 4˚C overnight. Samples were washed with PBS prior to incubation with fluorescein isothiocyanate- (1:500 dilution; cat nos. ab97063 and ab6881; Abcam) and Cy3- (1:500 dilution; cat no. ab97035; Abcam) labeled secondary antibodies for 1 h at room temperature. Subsequently, 1 μg/ml DAPI was used to stain for 10 min in the dark. Images were observed under a laser scanning confocal microscope (Olympus Corporation). For semi-quantitative morphometry, immunofluorescence staining was detected and calculated with ImageJ v1.42q software (NIH) in eight randomly selected micrographs.

Western blot analysis. Liver tissues were lysed in radioimmunoprecipitation assay buffer (P0013B; Beyotime Institute of Biotechnology, Shanghai, China), supplemented with protease inhibitor 1 mM phenylmethylsulfonyl fluoride for 30 min on ice and were centrifuged at 7,000 x g at 4˚C for 15 min. Protein concentration was detected by a spectrophotometer using a BCA protein assay kit according to the manufacturer's protocol. The protein samples (50 μg) were separated by 8-10% SDS-PAGE and were transferred to polyvinylidene difluoride membranes. Membranes were blocked in 5% BSA/PBS containing 0.1% Tween for 1 h at room temperature, and were then incubated with primary antibodies against E-cadherin (1:500 dilution; cat no. sc-7870), fibronectin (1:200 dilution; cat no. sc-69682) (both from Santa Cruz Biotechnology Inc.), collagen I (1:5,000 dilution; cat no. ab34710), Smad2/3 (1:500 dilution; cat no. ab217553), phosphorylated (p)-Smad2/3 (1:1,000 dilution; cat no. ab63399) and GAPDH (1:5,000 dilution; cat no. ab181602) (all from Abcam) at 4˚C overnight. GAPDH was used as an internal control. Horseradish
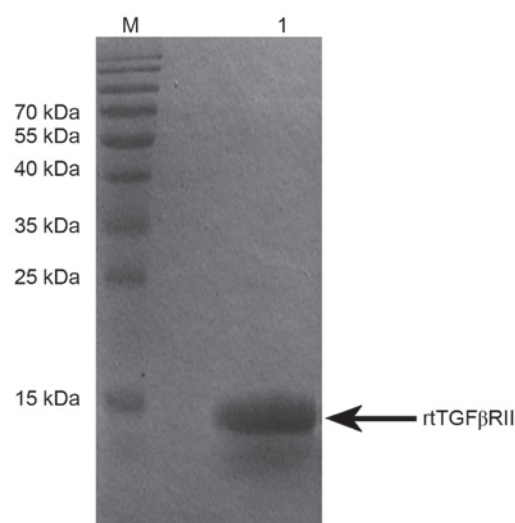

Figure 1. Expression and purification of rtTGFβRII in *Escherichia coli* BL21 cells by SDS-PAGE analysis. Lane M, protein marker; lane 1, rtTGFβRII purified protein. rtTGFβRII, recombinant truncated transforming growth factor β receptor II.

peroxidase-conjugated goat anti-rabbit IgG (1:5,000 dilution; cat no. ab97051) or goat anti-mouse IgG (1:5,000 dilution; cat no. ab97023) (both from Abcam) antibodies were used as secondary antibodies for 1 h at room temperature. Protein bands were detected using the 0.01% diaminobenzidine (cat no. PA110; Tiangen Biotech Co., Ltd., Beijing, China) chromogenic reagent and the signal intensity was semi-quantified using ImageJ v1.42q software (NIH).

Statistical analysis. The results of each experiment are representative of at least three independent experiments. Data were analyzed using a one-way analysis of variance with Tukey's multiple comparison test using GraphPad Prism 5.0 software (GraphPad Software, Inc., La Jolla, CA, USA) and were expressed as the mean ± standard error of the mean. P<0.05 was considered to indicate a statistically significant difference.

Results

Purification of rtTGFβRII protein. As shown in Fig. 1, the purified rtTGFβRII exhibited a single band following SDS-PAGE with Coomassie brilliant blue staining. The molecular weight of rtTGFβRII was ~13 kDa.

Activities of serum alanine aminotransferase (ALT) and aspartate aminotransferase (AST) activities. As shown in Fig. 2, the serum activities of ALT and AST were markedly increased (P<0.001) in the CCl$_4$ model group compared with those in the normal control group. Treatment with rtTGFβRII had a beneficial effect on ALT and AST activities; decreased ALT and AST activities (P<0.05) were detected in the CCl$_4$ + rtTGFβRII group compared with in the CCl$_4$ model group.

Histopathological alterations in the liver. H&E staining detected pathological alterations in the CCl$_4$ model group, including prominent hepatocyte degeneration, necrosis,
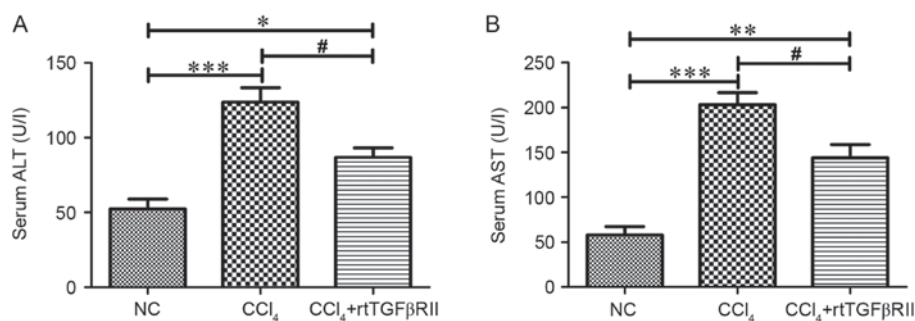
Figure 2. Effects of rtTGFβRII treatment on serum levels of ALT and AST in rat liver. Serum (A) ALT and (B) AST levels were measured by an automatic biochemical detector. Data are expressed as the mean ± standard error of the mean, n=8. *P<0.05, **P<0.01, ***P<0.001 compared with the NC group; #P<0.05 compared with the CCl$_4$ group. ALT, alanine aminotransferase; AST, aspartate aminotransferase; CCl$_4$, carbon tetrachloride; NC, normal control; rtTGFβRII, recombinant truncated transforming growth factor β receptor II.
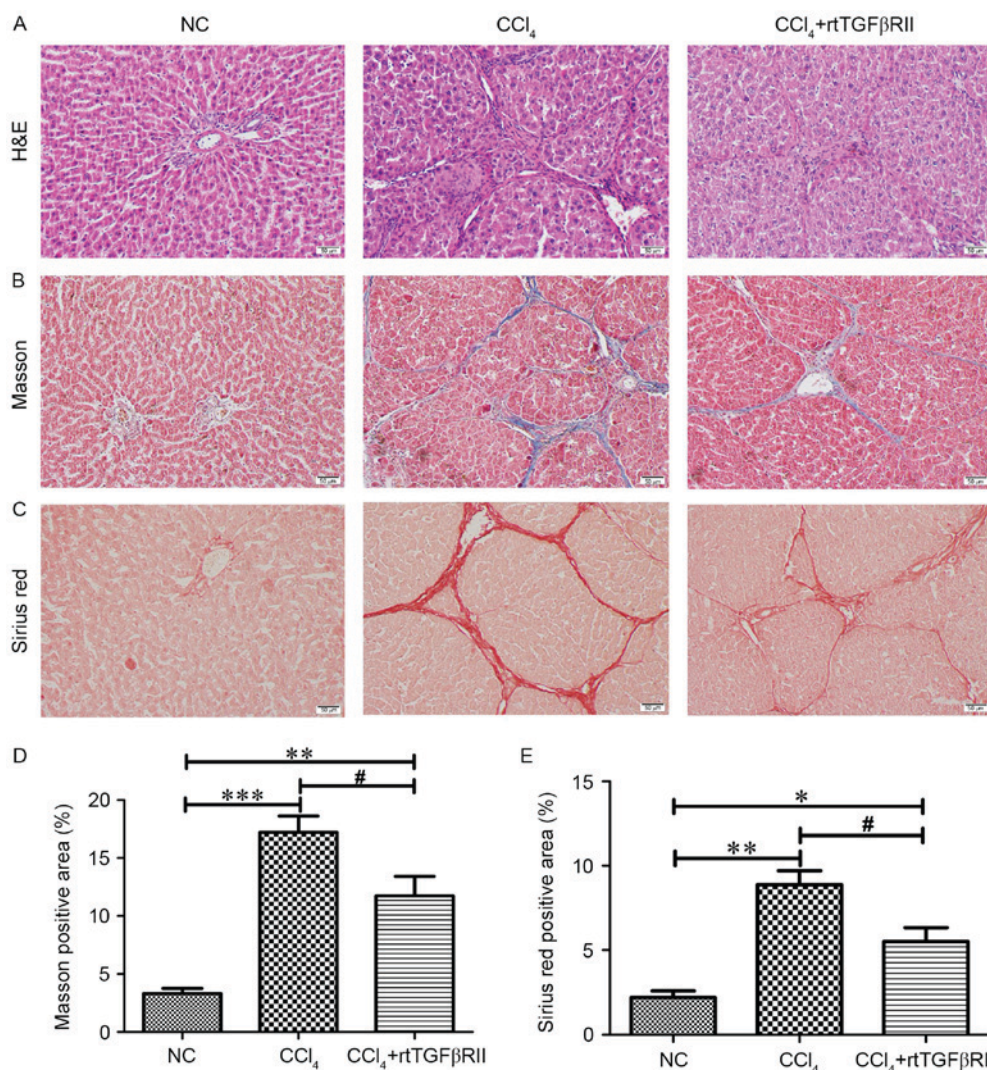

Figure 3. rtTGFβRII attenuates CCl$_4$-induced liver injury, fibrosis and collagen deposition. (A) H&E, (B) MTS and (C) Sirius red staining (magnification, x100) were performed on liver sections. Scale bars, 50 µm. (D and E) Semi-quantitative analysis for MTS and Sirius red staining, respectively. Data are presented as the mean ± standard error of the mean, n=8. *P<0.05, **P<0.01, ***P<0.001 compared with the NC group; #P<0.05 compared with the CCl$_4$ group. H&E, hematoxylin and eosin; MTS, Masson's trichrome; NC, normal control; rtTGFβRII, recombinant truncated transforming growth factor β receptor II.

inflammatory cell infiltration, periportal expansion and formation of pseudolobules (Fig. 3A). MTS and Sirius red staining detected a large amount of collagen fiber proliferation in the CCl$_4$ model group compared with in the NC group (Fig. 3B and C); however, and the surrounding fibrous tissue was significantly reduced (P<0.05) in the rtTGFβRII treatment group compared with the CCl$_4$ model group (Fig. 3D and E).
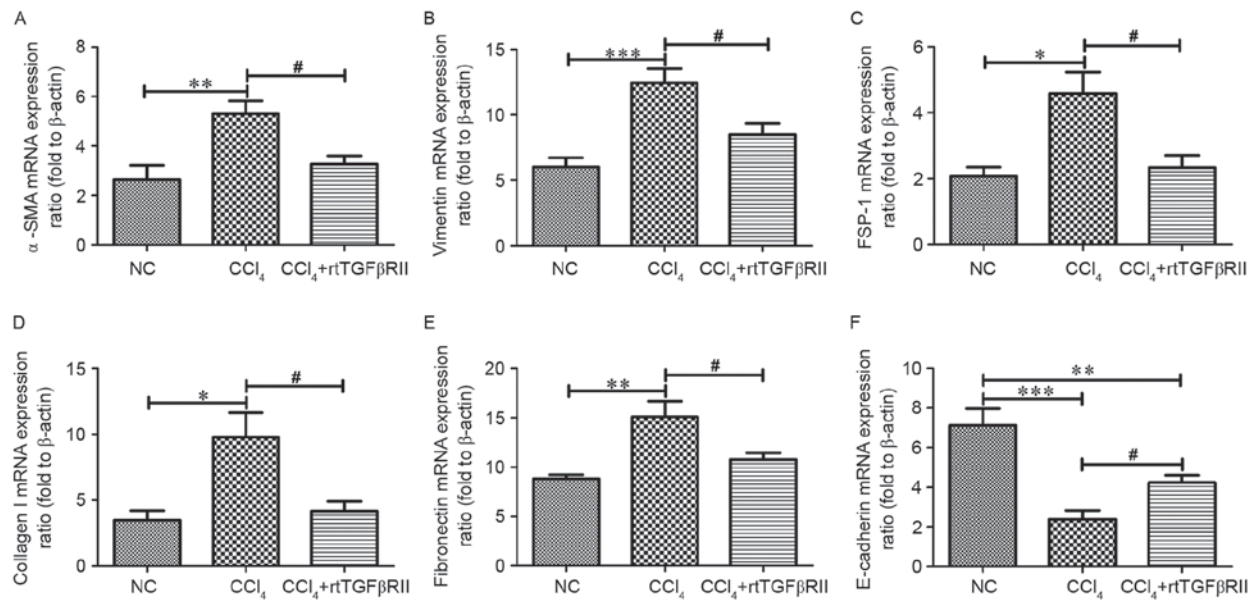
Figure 4. Effects of rtTGFβRII treatment on the mRNA expression levels of EMT markers. The mRNA expression levels of (A) α-SMA, (B) vimentin, (C) FSP-1, (D) collagen I, (E) fibronectin and (F) E-cadherin were detected by quantitative polymerase chain reaction analysis. mRNA expression levels were normalized to β-actin. Data are presented as the mean ± standard error of the mean, n=8. *P<0.05, **P<0.01, ***P<0.001 compared with the NC group; #P<0.05 compared with the CCl$_4$ group. α-SMA, α-smooth muscle actin; EMT, epithelial-mesenchymal transition; FSP-1, fibroblast specific protein-1; rtTGFβRII, recombinant truncated transforming growth factor β receptor II.

Effects of rtTGFβRII on ECM deposition and EMT expression in liver fibrosis. To evaluate whether rtTGFβRII modulates the accumulation of ECM and EMT expression in liver fibrosis, the mRNA expression levels of EMT-associated markers were investigated by RT-qPCR. A significant decrease in mRNA expression levels of the epithelial marker E-cadherin, and an increase in the mRNA expression levels of the mesenchymal cell markers fibronectin, α-SMA, vimentin, FSP-1 and collagen I were detected in the CCl$_4$ model group. However, rtTGFβRII treatment downregulated mesenchymal cell marker mRNA expression and slightly upregulated E-cadherin expression compared with the CCl$_4$ model group (Fig. 4). Immunofluorescence staining analysis indicated that the rtTGFβRII group exhibited reduced vimentin, α-SMA and fibronectin expression, and increased E-cadherin expression compared with the CCl$_4$ model group (Fig. 5). The present study further evaluated the expression of E-cadherin, collagen I, fibronectin and p-Smad2/3 via western blotting. There results demonstrated that collagen I, fibronectin and p-Smad2/3 protein levels were significantly higher in the CCl$_4$ model group compared with in the control group. Treatment with rtTGFβRII significantly decreased collagen I, fibronectin and p-Smad2/3 expression and increased the expression of E-cadherin (Fig. 6). The results indicated that rtTGFβRII could prevent the expression of fibroblast and mesenchymal markers, thus slowing down the progression of EMT in liver fibrosis.

Discussion

The present study is the first, to the best of our knowledge, to demonstrate that rtTGFβRII may ameliorate CCl$_4$-induced liver fibrosis through the inhibition of EMT. The anti-EMT effects of rtTGFβRII may be mediated by inhibition of TGF-β1 activation.

Liver fibrosis is marked by the accumulation of collagen and associated molecules in the liver. EMT is a process accompanied by a loss of epithelial markers, including E-cadherin, and a concurrent increase in mesenchymal and fibroblast markers, including α-SMA, collagens and FSP-1 (21,22). CCl$_4$ is widely used to generate animal models of liver fibrosis, and is a potent hepatotoxin that results in centrilobular hepatic necrosis (23). Altering the balance of ECM synthesis and degradation may be a key factor in the development of liver fibrosis (24). The role of TGF-β1 as a fibrogenic factor has been reported to trigger fibrogenesis. TGF-β1 promotes fibronectin and fibrillar collagens, inhibits ECM degradation through the expression of tissue inhibitors of matrix metalloproteinases and regulates ECM deposition. It has been demonstrated that myofibroblasts can be generated from parenchymal epithelial cells in the liver during fibrogenesis (25). In particular, it is accepted that hepatocyte EMT serves a key role in the perpetuation of liver fibrosis.

TGF-β is a highly pleiotropic cytokine. Mammals have three different forms of TGF-β: TGF-β1, TGF-β2 and TGF-β3 (26). These three TGF-βs bind to similar receptors: TGFβRI; TGFβRII and TGFβRIII, respectively (27,28). TGFβRI and TGFβRII are endowed with similar transmembrane serine/threonine kinases activity (29,30). In the TGF-β signaling pathway, signaling is initiated through binding to TGFβRII and TGFβRI serine/threonine kinases by active TGF-β1 ligands. This is a critical event in the TGF-β signaling pathway, which serves as the initiation point for downstream events.

TGF-β is considered a key mediator of fibrosis that induces EMT. TGF-β1 is an important cytokine that induces fibrosis and the profibrogenic pathway in the liver. Smad2/3 are important molecules of the TGF-β/Smad signaling
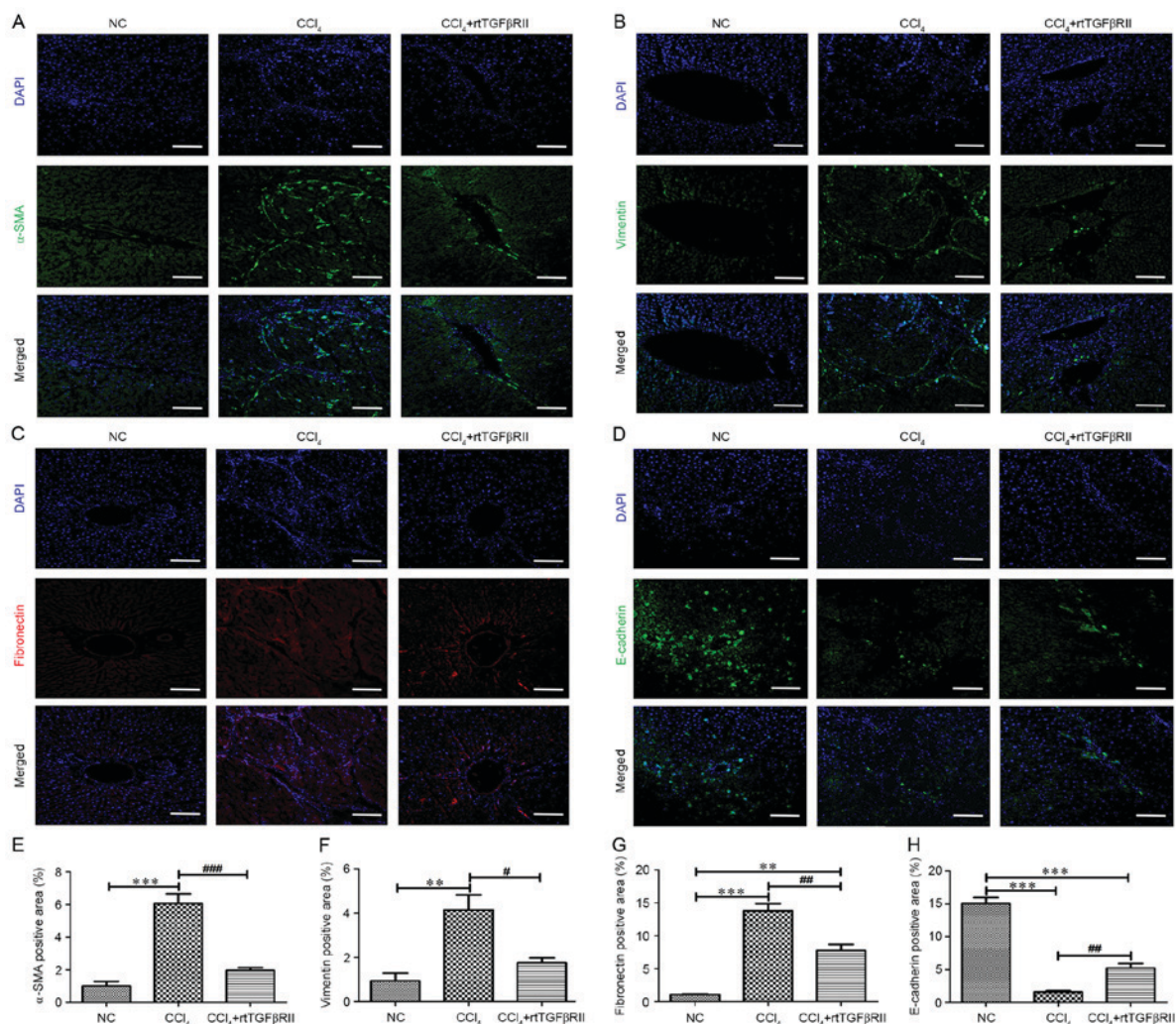
Figure 5. rtTGFβRII decreased CCl₄-induced α-SMA, vimentin, and fibronectin expression, and increased the expression of E-cadherin. Immunofluorescence staining (magnification, x100) was performed for (A) α-SMA, (B) vimentin, (C) fibronectin and (D) E-cadherin. Scale bars, 100 μm. (E-H) Semi-quantitative analysis for immunofluorescence staining. Data are presented as the mean ± standard error of the mean, n=8. **P<0.01, ***P<0.001 compared with the NC group; $^{#}$P<0.05, $^{##}$P<0.01, $^{###}$P<0.001 compared with the CCl₄ group. α-SMA, α-smooth muscle actin; rtTGFβRII, recombinant truncated transforming growth factor β receptor II.
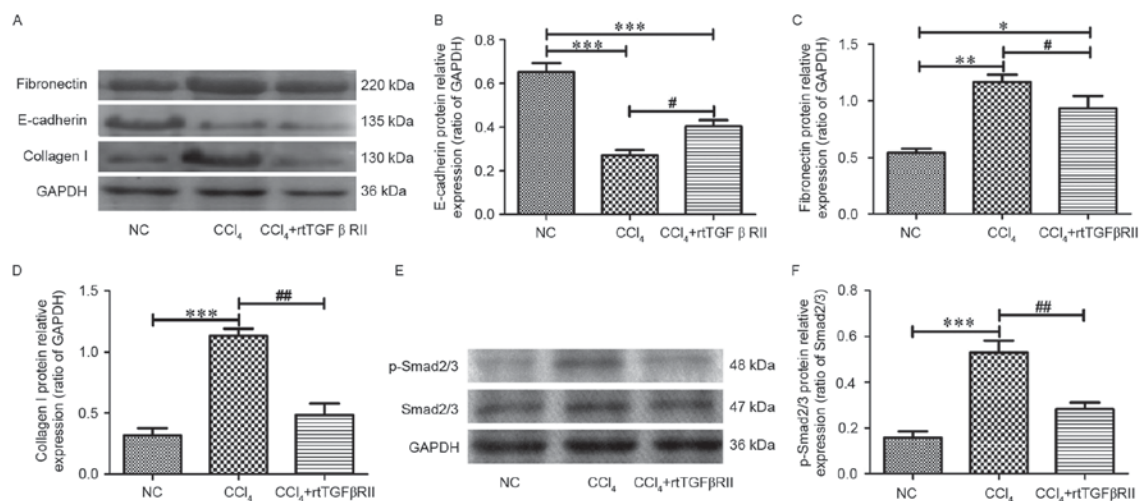

Figure 6. Effects of rtTGFβRII treatment on the protein expression of fibronectin, collagen I and E-cadherin, Smad2/3 and p-Smad2/3 in rat liver. (A) Western blot analysis of fibronectin, collagen I and E-cadherin protein levels. (B-D) Semi-quantitative data from densitometric analysis of fibronectin, collagen I and E-cadherin presented as the relative ratio of each protein to GAPDH. (E) Western blot analysis of p-Smad2/3 protein levels. (F) Semi-quantitative data from densitometric analysis of p-Smad2/3 presented as the relative ratio of protein to Smad2/3. Data are presented as the mean ± standard error of the mean of the optical density of each band, n=8. *P<0.05, **P<0.01, ***P<0.001 compared with the NC group; $^{#}$P<0.05, $^{##}$P<0.01 compared with the CCl₄ group. p-Smad2/3, phosphorylated Smad2/3; rtTGFβRII, recombinant truncated transforming growth factor β receptor II.

pathway. It has previously been suggested that overexpression of TGF-β1 is associated with chronic liver fibrosis in patients and in various animal disease models, whereas inhibition of TGF-β1 has been revealed to reduce the development of fibrosis in experimental animal disease models (31). TGFβRII is a member of the serine/threonine kinase receptor family that includes activin receptors. The cytoplasmic region of these receptors contains the apparent kinase domain. Active TGF-β binds to TGFβRII, triggering the kinase activity of the cytoplasmic domain that in turn activates TGFβRI. The truncated 27-123 residues of TGFβRII are a partial fragment of the TGFβRII extracellular domain, which can efficiently trap TGF-β1; however, a lack of a kinase domain achieves the purpose of blocking TGF-β1-triggered signals. Glutathione-S-transferase-pull down assays and a yeast two-hybrid screening experiment were performed to verify the affinity of tTGFβRII to TGF-β1. A previous study demonstrated that rtTGFβRII is able to bind to ligands and associates with TGFβRI, but is unable to activate TGFβRI (18), thus blocking TGF-β1 activation and achieving the purpose of treating liver fibrosis by inhibiting EMT.

The present study investigated the effects of rtTGFβRII on liver fibrosis using an experimental CCl4-induced rat model. The results demonstrated that rtTGFβRII exerted its effects by reducing the serum levels of ALT, AST and the degree of liver fibrosis in rats. Enzyme serum levels are markers of liver damage and are key biomarkers reflecting the degree of liver function and liver fibrosis. H&E, MTS and Sirius red staining indicated that treatment with rtTGFβRII could alleviate liver fibrosis. RT-qPCR, immunofluorescence staining and western blotting results also demonstrated that rtTGFβRII induced inhibition of ECM component deposition, which was associated with the reversion of EMT.

In conclusion, the results of the present study indicated that rtTGFβRII may alter the balance of EMT *in vivo* via the inhibition of TGF-β1 activation. Inhibition of TGF-β1 by rtTGFβRII may lead to the attenuation of liver fibrosis and improvement of liver function. This study demonstrated that rtTGFβRII may represent a novel therapeutic approach for the treatment of EMT-associated diseases.

Acknowledgements

References

1. Zhong W, Shen WF, Ning BF, Hu PF, Lin Y, Yue HY, Yin C, Hou JL, Chen YX, Zhang JP, *et al*: Inhibition of extracellular signal-regulated kinase 1 by adenovirus mediated small interfering RNA attenuates hepatic fibrosis in rats. Hepatology 50: 1524-1536, 2009.
2. Bataller R and Brenner DA: Liver fibrosis. J Clin Invest 115: 209-218, 2005.
3. Zhan YY, Wang JH, Tian X, Feng SX, Xue L and Tian LP: Protective effects of seed melon extract on CCl4-induced hepatic fibrosis in mice. J Ethnopharmacol 193: 531-537, 2016.
4. Friedman SL: Mechanisms of hepatic fibrogenesis. Gastroenterology 134: 1655-1669, 2008.
5. Liu Y, Yang P, Chen N, Lin S and Liu M: Effects of recombinant human adenovirus-p53 on the regression of hepatic fibrosis. Int J Mol Med 38: 1093-1100, 2016.
6. Chen X, Ying X, Zhang W, Chen Y, Shi C, Hou Y and Zhang Y: The hepatoprotective effect of fraxetin on carbon tetrachloride induced hepatic fibrosis by antioxidative activities in rats. Int Immunopharmacol 17: 543-547, 2013.
7. Choi SS and Diehl AM: Epithelial-to-mesenchymal transitions in the liver. Hepatology 50: 2007-2013, 2009.
8. Thenappan A, Li Y, Kitisin K, Rashid A, Shetty K, Johnson L and Mishra L: Role of transforming growth factor beta signaling and expansion of progenitor cells in regenerating liver. Hepatology 51: 1373-1382, 2010.
9. Fabris L and Strazzabosco M: Epithelial-mesenchymal interactions in biliary diseases. Semin Liver Dis 31: 11-32, 2011.
10. Lee SJ, Kim KH and Park KK: Mechanisms of fibrogenesis in liver cirrhosis: The molecular aspects of epithelial-mesenchymal transition. World J Hepatol 6: 207-216, 2014.
11. Pinzani M: Epithelial-mesenchymal transition in chronic liver disease: Fibrogenesis or escape from death? J Hepatol 55: 459-465, 2011.
12. Taura K, Iwaisako K, Hatano E and Uemoto S: Controversies over the epithelial-to-mesenchymal transition in liver fibrosis. J Clinical Med 5: pii: E9, 2016.
13. Wells RG: Fibrogenesis. V. TGF-beta signaling pathways. Am J Physiol Gastrointest Liver Physiol 279: G845-G850, 2000.
14. Verrecchia F and Mauviel A: Transforming growth factor-beta and fibrosis. World J Gastroenterol 13: 3056-3062, 2007.
15. Zavadil J and Böttinger EP: TGF-beta and epithelial-to-mesenchymal transitions. Oncogene 24: 5764-5774, 2005.
16. Fabregat I, Moreno-Càceres J, Sánchez A, Dooley S, Dewidar B, Giannelli G and Ten Dijke P; IT-LIVERConsortium: TGF-β signalling and liver disease. FEBS J 283: 2219-2232, 2016.
17. Shrestha N, Chand L, Han MK, Lee SO, Kim CY and Jeong YJ: Glutamine inhibits CCl4 induced liver fibrosis in mice and TGF-β1 mediated epithelial-mesenchymal transition in mouse hepatocytes. Food Chem Toxicol 93: 129-137, 2016.
18. Chu Y, Guo F, Li Y, Li X, Zhou T and Guo Y: A novel truncated TGF-beta receptor II downregulates collagen synthesis and TGF-beta I secretion of keloid fibroblasts. Connect Tissue Res 49: 92-98, 2008.
19. Institute for Laboratory Animal Research. Guide for the Care and Ue of Laboratory Animals. 8th edition. National Academy Press, Washington, DC, 2011.
20. Livak KJ and Schmittgen TD: Analysis of relative gene expression data using real-time quantitative PCR and the 2(-Delta Delta C(T)) method. Methods 25: 402-408, 2001.
21. Sicklick JK, Choi SS, Bustamante M, McCall SJ, Pérez EH, Huang J, Li YX, Rojkind M and Diehl AM: Evidence for epithelial-mesenchymal transitions in adult liver cells. Am J Physiol Gastrointest Liver Physiol 291: G575-G583, 2006.
22. Rygiel KA, Robertson H, Marshall HL, Pekalski M, Zhao L, Booth TA, Jones DE, Burt AD and Kirby JA: Epithelial-mesenchymal transition contributes to portal tract fibrogenesis during human chronic liver disease. Lab Invest 88: 112-123, 2008.
23. Chen S, Zou L, Li L and Wu T: The protective effect of glycyrrhetinic acid on carbon tetrachloride-induced chronic liver fibrosis in mice via upregulation of Nrf2. PLoS One 8: e53662, 2013.
24. He X, Lv R, Wang K, Huang X, Wu W, Yin L and Liu Y: Cytoglobin exhibits anti-fibrosis activity on liver in vivo and in vitro. Protein J 30: 437-446, 2011.
25. Gressner OA and Gao C: Monitoring fibrogenic progression in the liver. Clin Chim Acta 433: 111-122, 2014.
26. Prud'homme GJ: Pathobiology of transforming growth factor beta in cancer, fibrosis and immunologic disease, and therapeutic considerations. Lab Invest 87: 1077-1091, 2007.
27. Li MO, Wan YY, Sanjabi S, Robertson AK and Flavell RA: Transforming growth factor-beta regulation of immune responses. Ann Rev Immunol 24: 99-146, 2006.
28. Rubtsov YP and Rudensky AY: TGFbeta signalling in control of T-cell-mediated self-reactivity. Nat Rev Immunol 7: 443-453, 2007.
29. Massague J: TGFβ signalling in context. Nat Rev Mol Cell Biol 13: 616-630, 2012.
30. ten Dijke P and Hill CS: New insights into TGF-β-Smad signalling. Trends Biochem Sci 29: 265-273, 2004.
31. Wynn TA and Ramalingam TR: Mechanisms of fibrosis: Therapeutic translation for fibrotic disease. Nat Med 18: 1028-1040, 2012.